Kieran J. Sharkey · Carmen Fernandez ·
Kenton L. Morgan · Edmund Peeler ·
Mark Thrush · James F. Turnbull ·
Roger G. Bowers

Pair-level approximations to the spatio-temporal dynamics of epidemics on asymmetric contact networks

Abstract The process of infection during an epidemic can be envisaged as being transmitted via a network of routes represented by a contact network. Most differential equation models of epidemics are mean-field models. These contain none of the underlying spatial structure of the contact network. By extending the mean-field models to pair-level, some of the spatial structure can be contained in the model. Some networks of transmission such as river or transportation networks are clearly asymmetric, whereas others such as airborne infection can be regarded as symmetric. Pair-level models have been developed to describe symmetric contact networks. Here we report on work to develop a pair-level model that is also applicable to asymmetric contact networks. The procedure for closing the model at the level of pairs is discussed in detail. The model is compared against stochastic simulations of epidemics on asymmetric contact networks and against the predictions of the symmetric model on the same networks.

Keywords asymmetric contact networks · pair-wise models · SIR · closure approximations

K. J. Sharkey, R. G. Bowers
Division of Applied Mathematics, Department of Mathematical Sciences, M&O Building, The University of Liverpool, Liverpool, L69 7ZL
E-mail: k.j.sharkey@liv.ac.uk

K. L. Morgan
Department of Veterinary Clinical Science, The University of Liverpool

J.F. Turnbull
Institute of Aquaculture, University of Stirling

C. Fernandez
Department of Statistics, Lancaster University

M. Thrush, E. Peeler
Center for Environment Fisheries and Aquaculture Science

1 Introduction

Differential equation models can be a useful tool in understanding and predicting the course of epidemics. The models are often constructed entirely at the single node level - the so-called mean field models. More recently, differential equations at the pair level have been investigated [7,11,5,9,13]. These equations have the potential to carry some of the spatial structure of the underlying contact network. Pair-level models were used to investigate the outbreak of foot & mouth disease in the UK in 2001 [3].

Here we develop a pair-level differential equation model for an SIR (susceptible-infectious-removed) infection [1,4]. In particular we extend the scope of previous work in this area to allow for asymmetric contact networks.

Transportation networks generally have biased directionality. If the transportation of livestock were included in the contact structure underlying the 2001 foot & mouth epidemic, a model allowing for asymmetric links would be required. The symmetric model is only applicable to the period following the livestock movement ban.

Another instance in which asymmetric networks may arise is disease transmission via water. Many aquatic animal pathogens can spread between hosts through water. In flowing water such spread is obviously more probable in a downstream direction. Infected fish can also spread disease by moving around in the aquatic environment either in search of food and shelter or as part of a systematic migration. A model of asymmetric transmission therefore clearly has application to diseases of aquatic life forms and for waterborne diseases in general.

In the next section we quantify the global structure of asymmetric contact networks at the order of triples. In section 3 we discuss a closure approximation for differential equation models at the level of pairs on asymmetric contact networks. Sections 4 and 5 introduce a differential equation model to describe the global evolution of an SIR infection on an underlying asymmetric contact network. Sections 6 and 7 compare this SIR model with the special case of the model for symmetric networks. Finally we report on the results of numerical simulations.

2 General network properties

We consider a network of N nodes. Transmission of infection between these nodes is assumed to be via contacts of equal strength. The contact structure between the nodes is represented by an $N \times N$ matrix G such that:

$$G_{ij} = \begin{cases} 1 \text{ if there is contact from node } i \text{ to node } j \\ 0 \text{ otherwise} \end{cases} \tag{1}$$

We also suppose that there is no self-contact; $G_{ii} = 0$.

Using the bracket notation [ ] to be read as "the number of", we can count the number of (directed) pairs of nodes on the contact network:

$$[\text{pairs}] = \|G\| = nN \tag{2}$$

where $\|G\| \equiv \sum_{i,j} G_{ij}$. Equation (2) defines n, the average number of contacts or neighbours per node.

We now split the contact network G into a symmetric network $G_{\leftrightarrow}$ where all of the links are bidirectional and an asymmetric network $G_{\rightarrow}$ where all of the links are unidirectional:

$$
\begin{aligned}
(G_{\leftrightarrow})_{ij} &= G_{ij}G_{ji} \\
(G_{\rightarrow})_{ij} &= G_{ij}(1 - G_{ji})
\end{aligned}
\tag{3}
$$

so that $G = G_{\leftrightarrow} + G_{\rightarrow}$. We also specify the network of nodes with no direct contact (in either direction). We will refer to this as the open network $G_{\bowtie}$:

$$
(G_{\bowtie})_{ij} = 1 - (G_{\leftrightarrow} + G_{\rightarrow} + G_{\rightarrow}^T)_{ij} - \delta_{ij}
\tag{4}
$$

where δ_{ij} is the Kronecker delta. From these matrices we can define $n_{\leftrightarrow}, n_{\rightarrow}$, and $n_{\bowtie}$ to be the average number of symmetric, asymmetric and open neighbours per node respectively:

$$
\begin{aligned}
\|G_{\leftrightarrow}\| &= Nn_{\leftrightarrow} \\
\|G_{\rightarrow}\| &= Nn_{\rightarrow} \\
\|G_{\bowtie}\| &= Nn_{\bowtie}
\end{aligned}
\tag{5}
$$

From this it follows using equations (2), (3) and (4) that:

$$
n = n_{\leftrightarrow} + n_{\rightarrow}
\tag{6}
$$

and:

$$
n_{\bowtie} = N - 1 - n_{\leftrightarrow} - 2n_{\rightarrow}
\tag{7}
$$

Any ordered pair of nodes are linked by one of the networks $G_{\leftrightarrow}$, $G_{\rightarrow}$, $G_{\rightarrow}^T$ or $G_{\bowtie}$. Ignoring the completely open triple, this gives nine distinct ways in which triples can be arranged. These are shown in figure 1. Introducing the following arrow notation, we can count the total numbers of type a,b,c,d,e,f,g,h and i triples respectively as:

$$
\begin{aligned}
[\rightarrow\leftarrow \cdots] &= \|G_{\rightarrow}G_{\rightarrow}^T\| - Tr(G_{\rightarrow}G_{\rightarrow}^T) \approx Nn_{\rightarrow}(n_{\rightarrow} - 1) \\
[\leftarrow\rightarrow \cdots] &= \|G_{\rightarrow}^T G_{\rightarrow}\| - Tr(G_{\rightarrow}^T G_{\rightarrow}) \approx Nn_{\rightarrow}(n_{\rightarrow} - 1) \\
[\rightarrow\rightarrow \cdots] &= \|G_{\rightarrow}^2\| \approx Nn_{\rightarrow}^2 \\
[\rightarrow\leftrightarrow \cdots] &= \|G_{\rightarrow}G_{\leftrightarrow}\| \approx Nn_{\rightarrow}n_{\leftrightarrow} \\
[\leftarrow\leftrightarrow \cdots] &= \|G_{\rightarrow}^T G_{\leftrightarrow}\| \approx Nn_{\rightarrow}n_{\leftrightarrow} \\
[\leftrightarrow\leftrightarrow \cdots] &= \|G_{\leftrightarrow}^2\| - Tr(G_{\leftrightarrow}^2) \approx Nn_{\leftrightarrow}(n_{\leftrightarrow} - 1) \\
[\rightarrow\bowtie \cdots] &= \|G_{\rightarrow}G_{\bowtie}\| \approx Nn_{\rightarrow}n_{\bowtie} \\
[\leftarrow\bowtie \cdots] &= \|G_{\rightarrow}^T G_{\bowtie}\| \approx Nn_{\rightarrow}n_{\bowtie} \\
[\leftrightarrow\bowtie \cdots] &= \|G_{\leftrightarrow}G_{\bowtie}\| \approx Nn_{\leftrightarrow}n_{\bowtie}
\end{aligned}
\tag{8}
$$

In addition to the exact counts, equation (8) also gives an example of approximations to these quantities. It is easily seen that these approximations are exact in the case of a network in which where every node has exactly the same number of symmetric contacts and exactly the same number of asymmetric contacts. In general the accuracy of this approximation is dependent
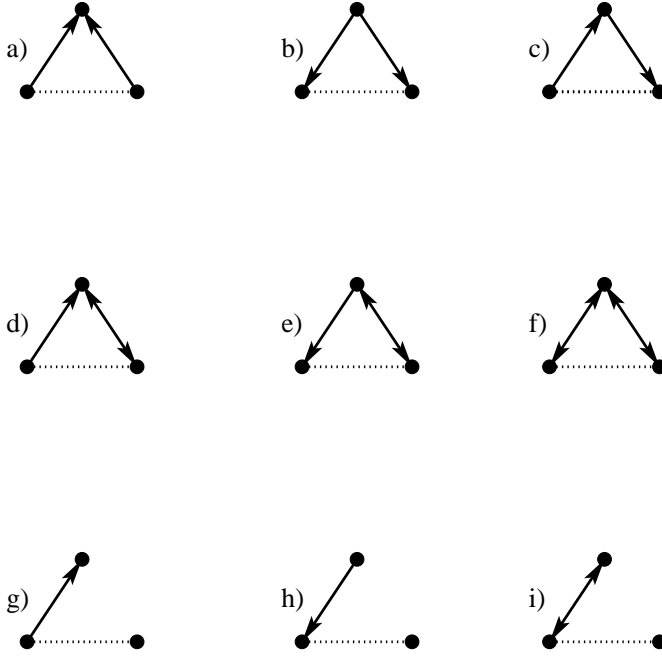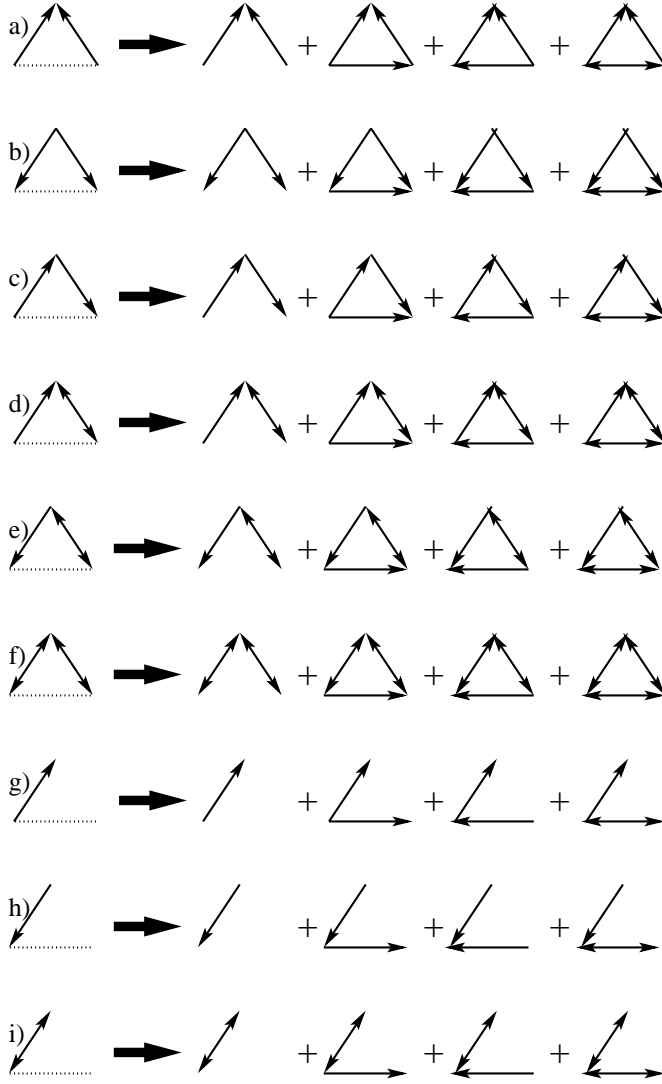
Fig. 1 This illustrates types of triples possible. The dotted lines indicate unspecified links so these could be via any of the networks $G_{\leftrightarrow}$, $G_{\rightarrow}$, $G_{\rightarrow}^{T}$ or $G_{\bowtie}$.

on the specific distribution in the number of neighbours per node. The validity of this kind of approximation is indirectly discussed by Rand [11] for different distributions. The results in the present paper do not depend on these approximations and we provide them here only draw comparisons with prior work on pair-approximations [11,5,9,13]. Approximations of this type may be useful in cases where the whole network is not known, but where the average number of neighbours per node may be estimated, perhaps by studying a subsection of the network.

The link represented by the dotted line in figure 1 is unspecified and so each of the nine triples can take four different forms. This decomposition is shown explicitly in figure 2. Many of the objects in figure 2 are copies of each other. There are seven distinct types of triple containing no open links. These can be counted on the network by:

$$
\begin{aligned}
c_1 &= [\rightarrow\leftarrow\leftarrow] = Tr(G_{\rightarrow}(G_{\rightarrow}^{T})^2) \\
c_2 &= [\rightarrow\leftrightarrow\leftarrow] = Tr(G_{\rightarrow}G_{\leftrightarrow}G_{\rightarrow}^{T}) \\
c_3 &= [\leftarrow\leftrightarrow\leftarrow] = Tr(G_{\rightarrow}^{T}G_{\leftrightarrow}G_{\rightarrow}^{T}) \\
c_4 &= [\leftrightarrow\leftrightarrow\rightarrow] = Tr(G_{\leftrightarrow}^{2}G_{\rightarrow}) \\
c_5 &= [\rightarrow\rightarrow\rightarrow] = Tr(G_{\rightarrow}^{3}) \\
c_6 &= [\leftarrow\leftrightarrow\rightarrow] = Tr(G_{\rightarrow}^{T}G_{\leftrightarrow}G_{\rightarrow}) \\
c_7 &= [\leftrightarrow\leftrightarrow\leftrightarrow] = Tr(G_{\leftrightarrow}^{3})
\end{aligned}
\tag{9}
$$

Fig. 2 Diagram of the triples in figure 1 including the closing links.

There are eight distinct types of triple containing either one or two open links. These can be counted on the network by:

$$
\begin{aligned}
o_1 &= [\rightarrow\leftarrow\bowtie] = Tr(G_\rightarrow G_\rightarrow^T G_\bowtie) = [\rightarrow\leftarrow\cdots] - 2c_1 - c_6 \\
o_2 &= [\leftarrow\rightarrow\bowtie] = Tr(G_\rightarrow^T G_\rightarrow G_\bowtie) = [\leftarrow\rightarrow\cdots] - 2c_1 - c_2 \\
o_3 &= [\rightarrow\rightarrow\bowtie] = Tr(G_\rightarrow^2 G_\bowtie) = [\rightarrow\rightarrow\cdots] - c_1 - c_5 - c_3 \\
o_4 &= [\rightarrow\leftrightarrow\bowtie] = Tr(G_\rightarrow G_\leftrightarrow G_\bowtie) = [\rightarrow\leftrightarrow\cdots] - c_2 - c_3 - c_4 \\
o_5 &= [\leftarrow\leftrightarrow\bowtie] = Tr(G_\rightarrow^T G_\leftrightarrow G_\bowtie) = [\leftarrow\leftrightarrow\cdots] - c_3 - c_6 - c_4 \\
o_6 &= [\leftrightarrow\leftrightarrow\bowtie] = Tr(G_\leftrightarrow^2 G_\bowtie) = [\leftrightarrow\leftrightarrow\cdots] - 2c_4 - c_7 \\
o_7 &= [\rightarrow\bowtie\bowtie] = Tr(G_\rightarrow G_\bowtie^2) = [\rightarrow\bowtie\cdots] - o_2 - o_3 - o_5 \\
o_8 &= [\leftrightarrow\bowtie\bowtie] = Tr(G_\leftrightarrow G_\bowtie^2) = [\leftrightarrow\bowtie\cdots] - o_5 - o_4 - o_6
\end{aligned}
\tag{10}
$$

where the final equalities follow from equations (4), (8) and (9) and are consistent with figure 2. Using these values we can write down a matrix M detailing the number of each of the triples in figure 2:

$$
M = \begin{pmatrix}
o_1 & c_1 & c_1 & c_6 \\
o_2 & c_1 & c_1 & c_2 \\
o_3 & c_1 & c_5 & c_3 \\
o_4 & c_2 & c_3 & c_4 \\
o_5 & c_3 & c_6 & c_4 \\
o_6 & c_4 & c_4 & c_7 \\
o_7 & o_2 & o_3 & o_5 \\
o_7 & o_3 & o_1 & o_4 \\
o_8 & o_5 & o_4 & o_6
\end{pmatrix}
\tag{11}
$$

Here each element of M corresponds to the triple in figure 2 in the same position. Notice, for example, that the second and third terms in figure 2a are structurally the same. However, both terms are required since they differ when the identities of the nodes are considered.

Equation (8) shows that the total number of triples can be approximated if the values of $n_\rightarrow$, $n_\leftrightarrow$, and $n_\bowtie$ can be estimated. In the absence of a complete network, the elements of matrix M could also be estimated by studying subsections of the network.

3 Closure approximations

Closure approximations are necessary to solve master equations which, in general, contain terms at an order one higher than that of interest. For example, the construction of soluble models at the single node level requires that the pair quantities are approximated in terms of single nodes. Likewise, soluble models at the pair level require approximations of triples at the level of pairs. In this section we will look at one way of forming these approximations.

Let us first look at the approximation of pair level quantities in terms of single nodes. Let $A, B, ...$ represent nodes in particular states. Let $a, b, ...$ denote the type of network bond. For this work, these bonds are typically $\leftrightarrow$, $\leftarrow$, $\rightarrow$, or $\bowtie$. We shall denote the number of type AB pairs on a network a by $[A \overset{a}{-} B]$. Let $P(A \overset{a}{-} B)$ denote the probability of picking an $A \overset{a}{-} B$ pair uniformly at random from the set of all pairs on network a. Then we have:

$$
[A \overset{a}{-} B] = [\overset{a}{-}]P(A \overset{a}{-} B)
\tag{12}
$$

where $[\overset{a}{-}]$ denotes the number of pairs on network a.

Let us now approximate this probability by assuming independence in the states of the nodes:

$$
P(A \overset{a}{-} B) \approx P(A)P(B)
\tag{13}
$$

We now define $P(A)$ as the probability of selecting a node in state A uniformly at random from the set of all nodes:

$$P(A \overset{a}{-} B) \approx \frac{[A][B]}{N^2} \tag{14}$$

Substituting this into equation (12) gives:

$$[A \overset{a}{-} B] \approx \frac{n_a[A][B]}{N} \tag{15}$$

where we have used the form of equation (2) to define n_a for any network a. This equation can be used to approximate pair-level quantities and generate mean-field models.

Now consider approximations for triples quantities. In the case of an asymmetric network, there is a complication since, as can be seen from figure 2, each triple occurs in four different forms. For the most accurate description, each of these forms has to be considered separately. This then takes into account the maximum available structure at the triples level. Referring to the triple illustrated in figure 2a, we have:

$$[A \to B \leftarrow C] = \quad [A \to B \leftarrow C \bowtie A] + [A \to B \leftarrow C \leftarrow A] \\ + [A \to B \leftarrow C \to A] + [A \to B \leftarrow C \leftrightarrow A] \tag{16}$$

where the correspondence between this notation and the relevant triples in the diagram should be clear. Here and in what follows, we use $[A \overset{a}{-} B \overset{b}{-} C]$ to mean $[A \overset{a}{-} B \overset{b}{-} C \cdots A]$.

We can approximate each of the terms in equation (16) by using an analogous argument to the mean field approximation. We start with the equivalent of equation (12):

$$[A \overset{a}{-} B \overset{b}{-} C \overset{c}{-} A] = [\overset{a\ b\ c}{-\,-\,-}]P(A \overset{a}{-} B \overset{b}{-} C \overset{c}{-} A) \tag{17}$$

Noting that the first row of the matrix in equation (11) gives the numbers of each of the types of triple in equation (16), then in conjunction with equation (17) we have:

$$[A \to B \leftarrow C] = \quad M_{11}P(A \to B \leftarrow C \bowtie A) + M_{12}P(A \to B \leftarrow C \leftarrow A) \\ + M_{13}P(A \to B \leftarrow C \to A) + M_{14}P(A \to B \leftarrow C \leftrightarrow A) \tag{18}$$

These matrix elements are precisely defined (see equations (9)-(11)) in terms of network properties. If insufficient details of this are known, they may be estimated.

To complete the triples approximation we need an approximation of the probabilities in equation (18) in terms of pair quantities. Figure 3 shows how a triple is formed by three pairs of nodes. The pairs in figure 3 are not independent of each other. In addition to higher order dependencies, the identity of a node in one pair specifies the identity of a node in another pair. The dashed arrows show this dependence in the structure in a symmetrical way. Referring to figure 3 and using the approximation of statistical independence
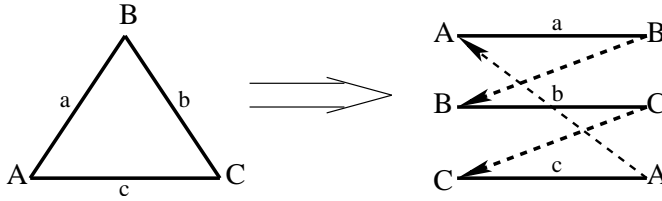
Fig. 3 This shows how a triple is composed of three pairs of nodes. The letters a, b and c indicate the type of link between the nodes. The dotted arrows show that the pairs share nodes in common.

at the level of pairs (this assumption underlies many of the pair approximations in the literature [7,11,9,13]) we have:

$$P(A \overset{a}{-} B \overset{b}{-} C \overset{c}{-} A) \approx P(A \overset{a}{-} B|A)P(B \overset{b}{-} C|B)P(C \overset{c}{-} A|C) \qquad (19)$$

where the quantity $P(A \overset{a}{-} B|A)$ is the probability that a neighbour (on network a) of node A chosen uniformly at random is of type B. It is given by the number of A nodes connected to B nodes divided by the number of A nodes connected to any node (see Morris [9]):

$$P(A \overset{a}{-} B|A) = \frac{[A \overset{a}{-} B]}{F_A^a} \qquad (20)$$

where we have defined:

$$F_A^a = \sum_X [A \overset{a}{-} X] \qquad (21)$$

where X runs over the complete set of available node states $A, B, \dots$.

Notice that equation (19) is generated by moving around the triangle in figure 3 in a clockwise direction. The result we obtain should be independent of the direction so we should get the same result in an anti-clockwise direction. However, equation (21) is not consistent with this. To satisfy this symmetry requirement, we shall instead use:

$$F_A^a \approx n_a[A] \qquad (22)$$

This is the assumption that the average number of neighbours of a node on a given network is independent of the state of that node.

Substituting the relevant triples densities into equation (18) gives:

$$[A \to B \leftarrow C] \approx \frac{[A \to B][B \leftarrow C]}{n_\to^2[A][B][C]} \left(M_{11} \frac{[C \bowtie A]}{n_\bowtie} + M_{12} \frac{[C \leftarrow A]}{n_\to} \right.$$
$$\left. + M_{13} \frac{[C \to A]}{n_\to} + M_{14} \frac{[C \leftrightarrow A]}{n_\leftrightarrow} \right) (23)$$

In a similar fashion, expressions for the other types of triple in figure 1 can be obtained.

It is important to be aware of the limitations of the type of approximation used in this section. The approximation contained in equation (19) assumes

that the state of a node depends only on the structure at the pair level and that higher order dependences are insignificant. It is difficult to know in advance of comparisons with simulations which networks will satisfy this assumption and which will not. For some networks this assumption turns out to be a bad one. For example, suppose that we have nodes uniformly distributed on a plane and each node is connected to its n spatially nearest neighbours. An epidemic on this network will tend to propagate outwards as a wave emanating from the first infected node. Models approximated at the level of pairs are very poor at predicting the course of epidemics on this type of network. A more relevant model for this is a diffusion equation model (see for example [8][10]). This type of local structure is of course present in triangular and square lattices.

4 An SIR model for asymmetric networks

We consider an epidemic model with susceptible, infectious and removed states which we denote by S, I, and R respectively. We assume that individuals in the removed state cannot return to susceptible or infectious states. In this model we also ignore birth and death processes.

By noting that the process of infection occurs via contact between an infectious node and a susceptible node, we can write down the rate of change of the numbers of nodes in each state:

$$
\begin{aligned}
[\dot{S}] &= -\tau[S \leftarrow I] - \tau[S \leftrightarrow I] \\
[\dot{I}] &= \tau[S \leftarrow I] + \tau[S \leftrightarrow I] - g[I]
\end{aligned}
\tag{24}
$$

where τ is the "rate" of infection across a link and g is the "rate" of removal of an infected individual. An equation for $[R]$ is not explicitly required as it is implied by having a complete set of states; $[S] + [I] + [R] = N$.

This system of equations is not closed. We can close the equations at the level of single nodes by approximating $[S \leftarrow I]$ and $[S \leftrightarrow I]$. Using equations (15) and (6) gives:

$$
[S \leftarrow I] + [S \leftrightarrow I] \approx \frac{n[S][I]}{N}
\tag{25}
$$

By using this approximation in equation (24) we close the system at the level of single nodes. This is an example of a "mean field" theory and is a special case of the Kermack-McKendrick model [6,2].

An alternative to closing the system at the level of single nodes is to write down further differential equations for the rates of change of the relevant

pair-level quantities. We have:

$$
\begin{aligned}
[S \overset{\cdot}{\to} S] \;=\; & -\tau[S \to S \leftarrow I] - \tau[I \to S \to S] \\
& -\tau[S \to S \leftrightarrow I] - \tau[I \leftrightarrow S \to S]
\end{aligned}
$$

$$
\begin{aligned}
[S \overset{\cdot}{\to} I] \;=\; & \tau[S \to S \leftarrow I] - \tau[I \to S \to I] - g[S \to I] \\
& +\tau[S \to S \leftrightarrow I] - \tau[I \leftrightarrow S \to I]
\end{aligned}
$$

$$
\begin{aligned}
[I \overset{\cdot}{\to} S] \;=\; & \tau[I \to S \to S] - \tau[I \to S \leftarrow I] - \tau[I \to S] - g[I \to S] \\
& +\tau[I \leftrightarrow S \to S] - \tau[I \to S \leftrightarrow I]
\end{aligned}
$$

$$
\begin{aligned}
[I \overset{\cdot}{\to} I] \;=\; & \tau[I \to S \to I] + \tau[I \to S \leftarrow I] + \tau[I \to S] - 2g[I \to I] \\
& +\tau[I \leftrightarrow S \to I] + \tau[I \to S \leftrightarrow I]
\end{aligned}
$$

$$
[S \overset{\cdot}{\leftrightarrow} S] = -2\tau[S \leftrightarrow S \leftarrow I] - 2\tau[S \leftrightarrow S \leftrightarrow I]
$$

$$
\begin{aligned}
[S \overset{\cdot}{\leftrightarrow} I] \;=\; & \tau[S \leftrightarrow S \leftarrow I] - \tau[I \to S \leftrightarrow I] - \tau[S \leftrightarrow I] - g[S \leftrightarrow I] \\
& +\tau[S \leftrightarrow S \leftrightarrow I] - \tau[I \leftrightarrow S \leftrightarrow I]
\end{aligned}
$$

$$
[I \overset{\cdot}{\leftrightarrow} I] \;=\; 2\tau[I \to S \leftrightarrow I] + 2\tau[I \leftrightarrow S \leftrightarrow I] + 2\tau[I \leftrightarrow S] - 2g[I \leftrightarrow I]
\tag{26}
$$

and for the open pairs:

$$
[S \overset{\cdot}{\bowtie} S] = -2\tau[S \bowtie S \leftarrow I] - 2\tau[S \bowtie S \leftrightarrow I]
$$

$$
[I \overset{\cdot}{\bowtie} I] = 2\tau[I \to S \bowtie I] + 2\tau[I \leftrightarrow S \bowtie I] - 2g[I \bowtie I]
\tag{27}
$$

$$
\begin{aligned}
[S \overset{\cdot}{\bowtie} I] = \; & \tau[S \bowtie S \leftarrow I] - \tau[I \to S \bowtie I] \\
& +\tau[S \bowtie S \leftrightarrow I] - \tau[I \leftrightarrow S \bowtie I] - g[S \bowtie I]
\end{aligned}
$$

These equations contain seven of the nine distinct types of triple identified in figure 1. To close these equations at the level of pairs, we use the approximations discussed in section 3.

5 Completeness relations

With the closure approximations in section 3, the differential equations (24), (26) and (27) can be solved. Here we show how to obtain a closed set of equations without using equation (27).

We have differential equations for a complete set of pairs. This was ensured by equation (4) and the construction of the open network. We can write the completeness relation for type AB pairs on an asymmetric network as:

$$
[A \cdots B] = [A \to B] + [A \leftarrow B] + [A \leftrightarrow B] + [A \bowtie B]
\tag{28}
$$

When A and B represent nodes in different states, we can determine the term on the left of this expression:

$$[A \cdots B] = \sum_{ij} A_i B_j = [A][B] \tag{29}$$

When the nodes are in the same state, we have:

$$[A \cdots A] = \sum_{ij} A_i A_j (1 - \delta_{ij}) = [A]^2 - \sum_{ij} A_i A_j \delta_{ij} \approx [A]^2 \left(1 - \frac{1}{N}\right) \tag{30}$$

where the approximation is almost exact. We use equation (30) instead of the more obvious expression $A(A-1)$ as it is consistent with equation (7) when the mean field approximations are substituted into equation (28) and is better suited to the continuous dynamics of differential equation models.

Differentiating equation (28) for different states and for the same state gives:

$$[A][\dot{B}] + [\dot{A}][B] = [A \xrightarrow{\cdot} B] + [A \xleftarrow{\cdot} B] + [A \xleftrightarrow{\cdot} B] + [A \bowtie\limits^{\cdot} B]$$
$$2[A][\dot{A}](1 - 1/N) = 2[A \xrightarrow{\cdot} A] + [A \xleftrightarrow{\cdot} A] + [A \bowtie\limits^{\cdot} A] \tag{31}$$

From equations (24),(26) and (27), we have expressions for each of these terms. By substituting these expressions into equation (31), it is easily seen that the terms in g are satisfied. That these equations are consistent in g is expected since equation (31) is exact (up to the approximation in equation (30)) and the dynamics of g are fully defined at the pair level. The terms in τ are also exact, but they are defined at the level of triples and their implementation in the model requires approximation at the level of pairs. The closure approximations in section 3 are a combination of triples level counts and pair-level dynamics. As such, these non-linear expressions cannot be shown to satisfy triples level identities in general. We shall encounter this issue again in section 7.

Notice that the completeness equations provide a simple way of calculating one of the types of pairs in terms of the others. For example by using the completeness relations, we do not need to solve equation (27) to calculate the open pairs. The difference between using this approach and solving equation (27) is negligible and is related to the issue of consistency just discussed. In numerical simulations presented in this paper, we always use the completeness relations for calculating open pairs.

We shall refer to the differential equations (24), (26) and the completeness relation (28), together with the closure approximations from section 3 as the "asymmetric" model.

6 Symmetric networks and node independence for open pairs

We notice now that in addition to the differential equations (equation (27)) and the completeness relations, there is a third way of determining the open pairs and so obtaining a complete system of equations. This is the assumption

of node independence that we used to derive the mean field approximation (equation (15)). Although not a pair level definition, in the case of open pairs it is likely to hold since these pairs do not interact directly with each other. We have $P(A \bowtie B) \approx P(A)P(B)$ so that:

$$[A \bowtie B] \approx \frac{n_{\bowtie}[A][B]}{N} \qquad (32)$$

For networks that are not highly connected it is also reasonable to write:

$$n_{\bowtie} \approx N$$
$$[A \bowtie B] \approx [A][B] \qquad (33)$$

We will now use this method for defining the open pairs to demonstrate the connection between the asymmetric model and the established triples approximations for symmetric networks [11,5,9,13].

For a symmetric network, equation (26) becomes:

$$[S \overset{\cdot}{\leftrightarrow} S] = -2\tau[S \leftrightarrow S \leftrightarrow I]$$
$$[S \overset{\cdot}{\leftrightarrow} I] = \tau[S \leftrightarrow S \leftrightarrow I] - \tau[I \leftrightarrow S \leftrightarrow I] - \tau[S \leftrightarrow I] - g[S \leftrightarrow I]$$
$$[I \overset{\cdot}{\leftrightarrow} I] = 2\tau[I \leftrightarrow S \leftrightarrow I] + 2\tau[I \leftrightarrow S] - 2g[I \leftrightarrow I] \qquad (34)$$

Furthermore $n_{\leftrightarrow} = n$ and all of the elements of M are zero except for M_{61}, M_{64}, M_{91} and M_{94}. With reference to the sixth row of figure 2, the triples approximation is then:

$$[A \leftrightarrow B \leftrightarrow C] \approx \frac{[A \leftrightarrow B][B \leftrightarrow C]}{n^2[A][B][C]} \left(M_{61}\frac{[C \bowtie A]}{n_{\bowtie}} + M_{64}\frac{[C \leftrightarrow A]}{n} \right) \quad (35)$$

If we now define ϕ to be the ratio of the number of triples with no open links to the total number of triples:

$$\phi = \frac{M_{64}}{[\leftrightarrow \leftrightarrow \cdots]} = \frac{M_{64}}{M_{61} + M_{64}} = \frac{Tr(G^3)}{\|G^2\| - Tr(G^2)} \qquad (36)$$

we can write:

$$[A \leftrightarrow B \leftrightarrow C] \approx N\zeta \frac{[A \leftrightarrow B][B \leftrightarrow C]}{[A][B][C]} \left((1-\phi)\frac{[C \bowtie A]}{n_{\bowtie}} + \phi\frac{[C \leftrightarrow A]}{n} \right) \qquad (37)$$

where $\zeta = [\leftrightarrow \leftrightarrow \cdots]/Nn^2$. Using node independence we can rewrite equation (37) in a more familiar form. Applying equation (33) for the open pair we have:

$$[A \leftrightarrow B \leftrightarrow C] \approx \zeta \frac{[A \leftrightarrow B][B \leftrightarrow C]}{[B]} \left((1-\phi) + \phi\frac{N[C \leftrightarrow A]}{n[A][C]} \right) \qquad (38)$$

This equation was first proposed by Morris[9] and is well known as a closure approximation for the pair-level dynamics on symmetric contact networks. However, we have a new definition of ζ. In other work, ζ is defined in terms of n. For example Keeling[5] uses $\zeta = (n-1)/n$. Notice that by using the approximations in equation (8), we find $\zeta = (n-1)/n$.

7 Comparison of the symmetric and asymmetric models

Here we look in more detail at the relationship between the asymmetric model and the special case of the model for symmetric networks. In particular it is of interest to determine how well a naive application of the simpler symmetric equations may perform in predicting epidemics on asymmetric contact networks.

It is useful to define the link $\Rightarrow$ to mean a connection between two nodes by either $\rightarrow$ or $\leftrightarrow$ so that:

$$[\Rightarrow] = [\leftrightarrow] + [\rightarrow] = \|G_\rightarrow\| + \|G_\leftrightarrow\| = \|G\| = Nn_\Rightarrow \qquad (39)$$

and:

$$[A \Rightarrow B] = [A \rightarrow B] + [A \leftrightarrow B] \qquad (40)$$

We also define the link $\nrightarrow$ to be either $\rightarrow$ or $\bowtie$. From equation (28) we then have the completeness relation:

$$[A \cdots B] = [A \Rightarrow B] + [A \nleftrightarrow B] \qquad (41)$$

and from equation (7) we have $n_\nrightarrow = n_\bowtie + n_\rightarrow = N - 1 - n_\Rightarrow$. Equation (41) can be used to define $[A \nleftrightarrow B]$ in terms of $[A \Rightarrow B]$ given equations (29) and (30).

We can use these definitions to generalise the closure approximation for symmetric networks (equation (37)):

$$[A \overset{a}{-} B \overset{b}{-} C] \approx \frac{[A \overset{a}{-} B][B \overset{b}{-} C]}{n_a n_b [A][B][C]} \left([\overset{a}{-}\overset{b}{-}\nleftrightarrow] \frac{[C \nleftrightarrow A]}{n_\nrightarrow} + [\overset{a}{-}\overset{b}{-}\Rightarrow] \frac{[C \Rightarrow A]}{n_\Rightarrow} \right)$$

$$= N\zeta_{ab} \frac{[A \overset{a}{-} B][B \overset{b}{-} C]}{[A][B][C]} \left((1 - \phi_{ab\Rightarrow}) \frac{[C \nleftrightarrow A]}{n_\nrightarrow} + \phi_{ab\Rightarrow} \frac{[C \Rightarrow A]}{n_\Rightarrow} \right) \qquad (42)$$

where:

$$\zeta_{ab} = \frac{\|G_a G_b\| - Tr(G_a G_b)}{Nn_a n_b}$$

$$\phi_{ab\Rightarrow} = \frac{Tr(G_a G_b G)}{\|G_a G_b\| - Tr(G_a G_b)} \qquad (43)$$

and it is understood that $G_\Rightarrow = G$. Note that equation (42) is exactly form equivalent to equation (37). Also the completeness relation (equation (41)) is exactly form equivalent to equation (28) when the asymmetric parts are removed. In the case of symmetric networks the closures are the same. In this sense it is a generalisation of the closure for symmetric networks.

Notice that equation (42) can also be written as:

$$[A \overset{a}{-} B \overset{b}{-} C] \approx N\zeta_{ab} \frac{[A \overset{a}{-} B][B \overset{b}{-} C]}{[A][B][C]} \left((1 - \phi_{ab\Leftarrow}) \frac{[A \nleftrightarrow C]}{n_\nrightarrow} + \phi_{ab\Leftarrow} \frac{[A \Rightarrow C]}{n_\Rightarrow} \right) \qquad (44)$$

with:

$$\phi_{ab\Leftarrow} = \frac{Tr(G_a G_b G^T)}{\|G_a G_b\| - Tr(G_a G_b)} \tag{45}$$

Either form of the closure is equally valid. However, when we come to apply this closure approximation to equations (46) and (51) below, it will be apparent that for these examples, equation (42) is more appropriate because it gives rise to terms in $[I \Rightarrow S]$ instead of $[S \Rightarrow I]$ and thereby leads to a closed system of equations.

Although the equations discussed in section 6 are only applicable to symmetric networks, it is interesting to ask how a "naive" application of them to asymmetric networks will perform. By a naive application we mean the way in which the model would behave if it were evaluated on an asymmetric instead of a symmetric network. We can write down this model as:

$$[\dot{S}] = -\tau[I \Rightarrow S]$$
$$[\dot{I}] = \tau[I \Rightarrow S] - g[I]$$
$$[S \overset{.}{\Rightarrow} S] = -2\tau[S \Rightarrow S \Rightarrow I]$$
$$[I \overset{.}{\Rightarrow} S] = \tau[S \Rightarrow S \Rightarrow I] - \tau[I \Rightarrow S \Rightarrow I] - \tau[I \Rightarrow S] - g[I \Rightarrow S]$$
$$[I \overset{.}{\Rightarrow} I] = 2\tau[I \Rightarrow S \Rightarrow I] + 2\tau[I \Rightarrow S] - 2g[I \Rightarrow I] \tag{46}$$

where we use the generalised closure (equation (42)) to define the triples quantities with:

$$\zeta_{\Rightarrow\Rightarrow} = \frac{\|G^2\| - Tr(G^2)}{Nn^2}$$
$$\phi_{\Rightarrow\Rightarrow\Rightarrow} = \frac{Tr(G^3)}{\|G^2\| - Tr(G^2)} \tag{47}$$

Since this model is designed for symmetric networks and makes no attempt to account for asymmetric structure other than the use of the asymmetric network G in equation (47), we shall refer to it as the "symmetric" model in the remainder of this paper.

Now look at the differential equations of the asymmetric model. Using equation (40), equation (24) becomes:

$$[\dot{S}] = -\tau[I \Rightarrow S]$$
$$[\dot{I}] = \tau[I \Rightarrow S] - g[I] \tag{48}$$

This is immediately seen to be the same as the $[S]$ and $[I]$ equations of the symmetric model.

By using triples level identities such as:

$$[A \Rightarrow B \Leftarrow C] = [A \rightarrow B \leftarrow C] + [A \rightarrow B \leftrightarrow C] + [A \leftrightarrow B \leftarrow C] + [A \leftrightarrow B \leftrightarrow C] \tag{49}$$

the $[S \rightarrow S]$, $[S \leftrightarrow S]$, $[I \rightarrow S]$, $[I \leftrightarrow S]$, $[I \rightarrow I]$ and $[I \leftrightarrow I]$ expressions in equation 26 can be reduced to:

$$[S \overset{\cdot}{\Rightarrow} S] = -\tau[S \Rightarrow S \Leftarrow I] - \tau[I \Rightarrow S \Rightarrow S]$$
$$[I \overset{\cdot}{\Rightarrow} S] = \ \ \tau[I \Rightarrow S \Rightarrow S] - \tau[I \Rightarrow S \Leftarrow I] - \tau[I \Rightarrow S] - g[I \Rightarrow S]$$
$$[I \overset{\cdot}{\Rightarrow} I] = \ \ \tau[I \Rightarrow S \Rightarrow I] + \tau[I \Rightarrow S \Leftarrow I] + \tau[I \Rightarrow S] + \tau[S \leftrightarrow I] - 2g[I \Rightarrow I]$$
$$(50)$$

The form of these equations is very similar to pair level expressions of the symmetric model. Motivated by this similarity, we define the following model:

$$[\overset{\cdot}{S}] = -\tau[I \Rightarrow S]$$
$$[\overset{\cdot}{I}] = \tau[I \Rightarrow S] - g[I]$$
$$[S \overset{\cdot}{\Rightarrow} S] = -\tau[S \Rightarrow S \Leftarrow I] - \tau[S \Leftarrow S \Leftarrow I]$$
$$[I \overset{\cdot}{\Rightarrow} S] = \tau[S \Leftarrow S \Leftarrow I] - \tau[I \Rightarrow S \Leftarrow I] - \tau[I \Rightarrow S] - g[I \Rightarrow S]$$
$$[I \overset{\cdot}{\Rightarrow} I] = \tau[I \Leftarrow S \Leftarrow I] + \tau[I \Rightarrow S \Leftarrow I] + \gamma\tau[I \Rightarrow S] - 2g[I \Rightarrow I] \ (51)$$

where $\gamma = 1 + n_{\leftrightarrow}/n$. These equations are closed by equation (42) and use $\zeta_{\Leftarrow\Leftarrow} = \zeta_{\Rightarrow\Rightarrow}$ and:

$$\zeta_{\Rightarrow\Leftarrow} = \frac{\|GG^T\| - Tr(GG^T)}{Nn^2}$$
$$\phi_{\Rightarrow\Leftarrow\Rightarrow} = \frac{Tr(G^2G^T)}{\|GG^T\| - Tr(GG^T)}$$
$$\phi_{\Leftarrow\Leftarrow\Rightarrow} = \frac{Tr(G^2G^T)}{\|G^2\| - Tr(G^2)}$$
$$(52)$$

which are obtained from equation (43).

We refer to this as the "part-asymmetric" model. Comparison of equations (46) and (51) suggests that it better accounts for the asymmetry than the symmetric model. It does, however, differ from the fully asymmetric model in the following three ways (the effect of these will be investigated numerically in the next section):

- The differential equations for the models are the same except for the $[I \Rightarrow I]$ expression where we have replaced $[I \Rightarrow S] + [I \leftrightarrow S]$ in the asymmetric model by $\gamma[I \Rightarrow S]$. This is the assumption that the proportion of IS pairs on symmetric links is the same as the proportion on asymmetric links; $[I \leftrightarrow S]/[\leftrightarrow] = [I \rightarrow S]/[\rightarrow]$. The $[I \Rightarrow I]$ expression is only required for the detailed triples structure in the $[I \Rightarrow S \Leftarrow I]$ term and it is not needed at all for networks with no closed triples. Clearly the sensitivity of the model to the value of γ will depend on the number of closed triples in the network.

– Another difference is related to the closure of the differential equations. From section (3), a general ABC triple is approximated in the asymmetric model by:

$$[A \overset{a}{-} B \overset{b}{-} C] \approx \frac{[A \overset{a}{-} B][B \overset{b}{-} C]}{n_a n_b [A][B][C]} \left([\overset{a}{-}\overset{b}{-}\bowtie] \frac{[C \bowtie A]}{n_\bowtie} + [\overset{a}{-}\overset{b}{-}\leftarrow] \frac{[C \leftarrow A]}{n_\rightarrow} \right.$$
$$\left. + [\overset{a}{-}\overset{b}{-}\rightarrow] \frac{[C \rightarrow A]}{n_\rightarrow} + [\overset{a}{-}\overset{b}{-}\leftrightarrow] \frac{[C \leftrightarrow A]}{n_\leftrightarrow} \right) \tag{53}$$

As we observed at the end of section 5, this approximation is non-linear. Because of this, while linear triples level expressions such as equation (49) must be true, pair-level approximations to the triples cannot be shown to satisfy these expressions in general. Consequently, equation (50) when closed with equation (53) cannot be shown to follow from the closed version of equation (26). However, given that the triples approximations are well-conceived, they should perform satisfactorily numerically.

– For the closure of equation (51), we use the less detailed equation (42) in place of equation (53). This lack of detail will lead to differences in the models on some networks. Conditions under which the closures are expected to differ can be determined, but due to the other differences, this analysis is not relevant.

By comparing the part-asymmetric and symmetric models, it is straightforward to write down the conditions under which they are the same. By comparing equation (46) with equation (51), it is clear that we need $\gamma = 2$. We quantify this condition as $\Gamma = 0$ where:

$$\Gamma \equiv (2 - \gamma) \frac{Tr(G^3) + Tr(G^2 G^T)}{\|G^2\| - Tr(G^2)} \tag{54}$$

Here the multiplicative fraction in terms of G is a measure of the number of closed triples in the network. This factor is included to account for the fact that for networks with no triangles, the value of γ is not important.

By comparing equations (47) and (52), the other necessary conditions are seen to be $\alpha = 0$ and $\theta = 0$ where:

$$\alpha \equiv |\zeta_{\Rightarrow\Rightarrow} - \zeta_{\Rightarrow\Leftarrow}| \tag{55}$$

and:

$$\theta \equiv \frac{\left| Tr(G^3) - Tr(G^2 G^T) \right|}{\|G^2\| - Tr(G^2)} \tag{56}$$

where the denominator is included to ensure that θ is between 0 and 1 and that it is very small for networks with few triangles.

The necessary and sufficient conditions for the symmetric and part-asymmetric models to be equivalent are:

$$\Gamma = 0$$
$$\alpha = 0$$
$$\theta = 0 \tag{57}$$

For a network that satisfies the approximations in equation (8), it can be shown that:

$$\alpha \approx \frac{n_{\rightarrow}}{n^2} \tag{58}$$

According to this, the condition $\alpha = 0$ is satisfied for purely symmetric networks and approximately satisfied for networks with large n.

From the analysis in this section we conclude that deviation between the symmetric and asymmetric models is likely to occur for asymmetric networks with small values of n. More generally, significant deviation is expected when the conditions in equation (57) are not approximately true. Beyond this, deviation may occur due to the difference between the asymmetric and part-asymmetric models discussed above. These observations assist in explaining the numerical results in the next section.

8 Numerical Results

Here we make numerical comparisons between the following four models:

– **Mean-Field Model**
  This model was discussed in section 4 and is composed of equation (24) together with the closure in equation (25). This model contains no spatial structure information apart from the average number of contacts per node; n.
– **Symmetric Model**
  This model was defined in section 7 and consists of equation (46) together with the closure (equation 42) and the completeness relation (equation (41)). The connection between this model and the symmetric model commonly found in the literature is discussed for symmetric networks in section 6.
– **Part-Asymmetric Model**
  This model was discussed in section 7 and consists of equation (51) together with the closure (equation (42)) and the completeness relation (equation 41). This simplified form contains some of the structure of the asymmetric model.
– **Asymmetric Model**
  This is the full asymmetric model consisting of the differential equations (24), (26) and the completeness relation (28), together with the closure approximations from section 3.

To solve these models we need to specify initial conditions. If $[I]_0$ is the initial number of infected individuals at time zero, then the initial condition for the susceptible population is $[S]_0 = N - [I]_0$. The initial conditions for the pair quantities are then obtained by the mean-field approximation (equation (15)).

These four models are compared against each other on four contact networks each with 8000 nodes. The networks are generated as follows:

– **Network 1(Random)**

An 8000×8000 matrix of uniformly random numbers between 0 and 1 is generated. Those elements that are less than or equal to $n/N = 6/8000$ are changed to have value 1 and all the other elements set equal to zero. As self interaction is not permitted, all diagonal elements are set equal to zero.

– **Network 2 (Random with triangles)**
An 8000×8000 random network is generated exactly as for network 1 except with $n = 5$. Calling this network G, we now construct the network $G + GG^T$. We put all diagonal elements equal to zero and make any element with a value greater than 1 equal to 1. This construction is a direct method of making a network with a higher density of triangles of transmission. The term GG^T turns open triples in the network G into triangles.

– **Network 3 (River)**
This network is motivated by considering the structure of river networks. The main way in which its structure differs from real river networks is that the "rivers" can move randomly between any nodes instead of moving in a generally consistent direction towards the sea. We construct it as follows: Starting with 8000 unconnected nodes, a node X is chosen uniformly at random from the 8000 nodes; X is connected to a different node Y chosen uniformly at random form the set of all nodes excluding X; Y in turn is connected to another node Z chosen uniformly at random from the set of all nodes excluding Y and so on until the chain is terminated. For each link on the chain, a random number between 0 and 1 is generated and if this number is less than $1/40$ then the chain is terminated. In this way, 300 such chains were generated. This produces a network of 300 "rivers" with a typical length of 40 nodes. When two nodes are connected more than once, the link in the network matrix has the value 1. This procedure results in a network with no diagonal elements.

– **Network 4 (Small world)**
This is motivated by the small world network discussed by Watts & Strogatz [14]. We start with 8000 nodes arranged regularly around a ring. This structure means that a given node has pairs of nodes equidistant from it around the ring (one clockwise and the other anticlockwise). We choose a node and then connect it to its nearest clockwise neighbour. The link is directed from the original node towards its neighbour. We also connect the node to its second and third nearest clockwise neighbours. Moving around the ring in a consistent direction we then repeat this for all 8000 nodes.

We now reconnect 20% of the links so as to introduce long range transmission. Starting from one of the nodes, we take the connection to its nearest clockwise neighbour and with probability 0.2, we reconnect this to another node chosen uniformly at random. If a link already exists between the two nodes, then the original link is left in place. We repeat this process for all nodes moving in a clockwise sense around the ring. This procedure is then repeated for the second and then the third nearest clockwise neighbours. This procedure produces a network with no symmetric links and no diagonal elements.
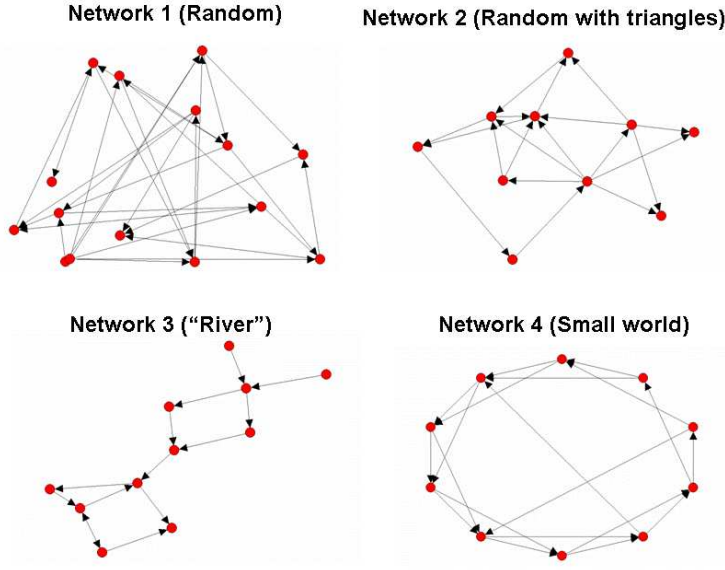
Fig. 4 Figure illustrating the structure in the four networks.

To give an impression of the structure of these networks, small scale examples are shown in figure 4. It may also be instructive to consider the matrix in equation (11), particularly with reference to figure (2). The top six rows of this matrix are given in equation (59) by M_1, M_2, M_3 and M_4 for networks 1,2,3 and 4 respectively:

$$
M_1 = 10^3 \times \begin{pmatrix} 284 & 0.23 & 0.23 & 0 \\ 285 & 0.23 & 0.23 & 0 \\ 285 & 0.23 & 0.25 & 0 \\ 0.19 & 0 & 0 & 0 \\ 0.18 & 0 & 0 & 0 \\ 0 & 0 & 0 & 0 \end{pmatrix}
\quad
M_2 = 10^3 \times \begin{pmatrix} 2581 & 267 & 267 & 0 \\ 2795 & 267 & 267 & 0 \\ 1979 & 267 & 2.90 & 0 \\ 0 & 0 & 0 & 0 \\ 0 & 0 & 0 & 0 \\ 0 & 0 & 0 & 0 \end{pmatrix}
$$

$$(59)$$

$$
M_3 = 10^3 \times \begin{pmatrix} 19.1 & 0.01 & 0.01 & 0 \\ 19.0 & 0.01 & 0.01 & 0 \\ 31.1 & 0.01 & 0.01 & 0 \\ 0.01 & 0 & 0 & 0 \\ 0 & 0 & 0 & 0 \\ 0 & 0 & 0 & 0 \end{pmatrix}
\quad
M_4 = 10^3 \times \begin{pmatrix} 32.0 & 12.3 & 12.3 & 0 \\ 23.4 & 12.3 & 12.3 & 0 \\ 59.7 & 12.3 & 0 & 0 \\ 0 & 0 & 0 & 0 \\ 0 & 0 & 0 & 0 \\ 0 & 0 & 0 & 0 \end{pmatrix}
$$

These matrices provide the detailed structure of the networks at the level of triples.

The four models were compared against stochastic simulations of epidemics on each of the contact networks. The simulations treat τ as the transmission probability per unit time and g as the recovery probability per unit

time. All epidemic simulations were initiated by a single infected individual ($[I]_0 = 1$).

Notice that the equations for each of the four models can be written in a non-dimensionalised form by applying the transformation:

$$
\begin{aligned}
t' &= t/g \\
\tau' &= \tau/g \\
g' &= 1
\end{aligned}
\tag{60}
$$

where t denotes time. This form demonstrates that by varying the single parameter τ', we obtain the full range of behaviours of the equations. To vary τ' we hold g fixed at $g = 0.05$ and vary τ. A range for τ is determined by using R_0 from mean-field theory as a guide:

$$
R_0^{\mathrm{mf}} = \frac{\beta}{g} = \frac{n\tau}{g}
\tag{61}
$$

where we have assumed that $\tau = \beta/n$ where β is the contact parameter. We investigate the range of values $1.1 \leq R_0^{\mathrm{mf}} \leq 20$ using the end points and eight equally spaced intermediate ones. This gives τ in the range $0.0505/n \leq \tau \leq 1/n$.

Stochastic simulations of epidemics with $R_0 > 1$ produce either a major epidemic or result in early stochastic fade out. In the networks considered here the difference in the final size of the susceptible populations between the two types of behaviour is obvious. For deterministic differential equation models there can be no stochastic fade out and if $R_0 > 1$, a major epidemic must occur. Consequently it is only meaningful to compare the differential equation models to major outbreaks. We therefore rejected any simulation that resulted in stochastic fade out. For each value of τ we obtained 200 stochastic simulations of major epidemics, each one initiated at a node selected uniformly at random from the 8000 nodes. In figures 5 to 8, the mean of the 200 simulations is plotted with error bars indicating a single standard deviation.

For $R_0 > 1$, the probability of a major epidemic is given by $1 - 1/R_0$ (see, for example, section 10.3.3 of Renshaw [12]). Using this naively and approximating R_0 by R_0^{mf} suggests that for $R_0^{\mathrm{mf}} = 1.1$, only 9% of infections will result in a major epidemic. In practice, on the networks considered here, the probability of producing an epidemic for the $R_0^{\mathrm{mf}} = 1.1$ case is found to be very much less that 9%. It appears that the real R_0 is less than 1 so the plots in figures 5 to 8 corresponding to $R_0^{\mathrm{mf}} = 1.1$ indicate that there is no epidemic.

The results from the epidemic simulations are plotted against the predictions from each of the four differential equation models (figures 5 to 8). For the purposes of plotting, particular cuts of the simulation data were taken. These are:

- **a)** The full susceptible time series for τ corresponding to $R_0^{\mathrm{mf}} = 4.8$.
- **b)** The full infectious time series for τ corresponding to $R_0^{\mathrm{mf}} = 4.8$.
- **c)** The final size of the susceptible population against τ.
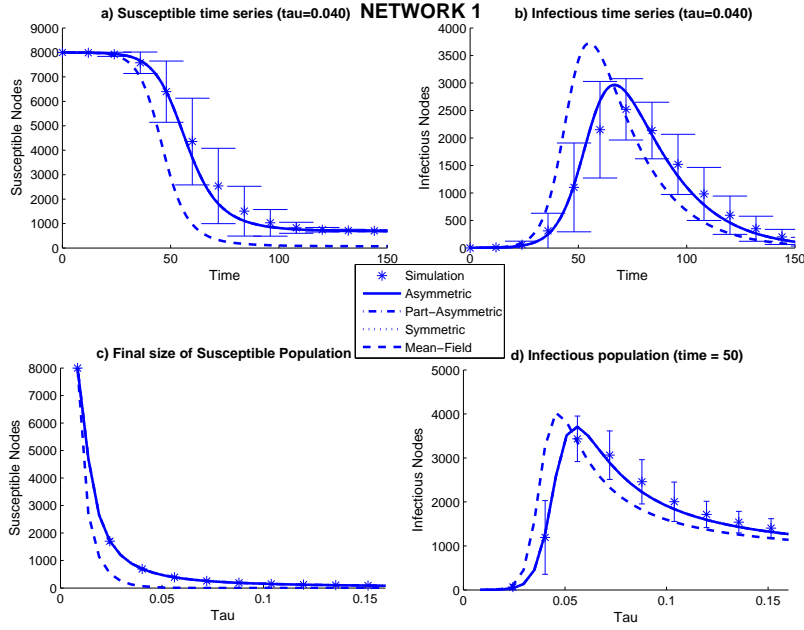
Fig. 5 (Random) This figure shows the simulation results and model predictions for the random network. The mean of 200 simulations is plotted with an asterix where the error bars on the plots indicate a single standard deviation. The other lines indicate the predictions of the four models, but only the mean-field prediction can be distinguished from the other three. The four graphs are: **a)**Susceptible time series for $\tau = 0.04$, $g = 0.05$, **b)**Infectious time series for $\tau = 0.04$, $g = 0.05$, **c)**Final size of the susceptible population and **d)**Infectious population at time interval 50.

Network	$n_{\rightarrow}$	$n_{\leftrightarrow}$	α	θ	Γ
Random	5.97	0.00	0.00	0.00	0.00
Random with triangles	17.29	0.00	0.36	0.12	0.12
River	1.54	0.00	0.63	0.00	0.00
Small world	3.00	0.00	0.21	0.17	0.17

Table 1 Table shows the network properties $n_{\rightarrow}$, $n_{\leftrightarrow}$, α, θ, and Γ for each of the four networks considered.

 – **d)** The number of infected individuals at time 50 against τ.

   In section 7 we discussed some network values that were useful in comparing the different models. These values are given for each network in table 1. We now discuss the results for each network in turn with reference to the values in table 1:

 – **Network 1(Random)**We see from figure 5 that (up to the resolution of the graph) the symmetric, part-asymmetric and asymmetric models cannot be distinguished. From equation (59) we see that there are very few closed triples on this network. This explains the near-zero values of θ and Γ given in table 1. Comparing the results for α, θ and Γ in table 1
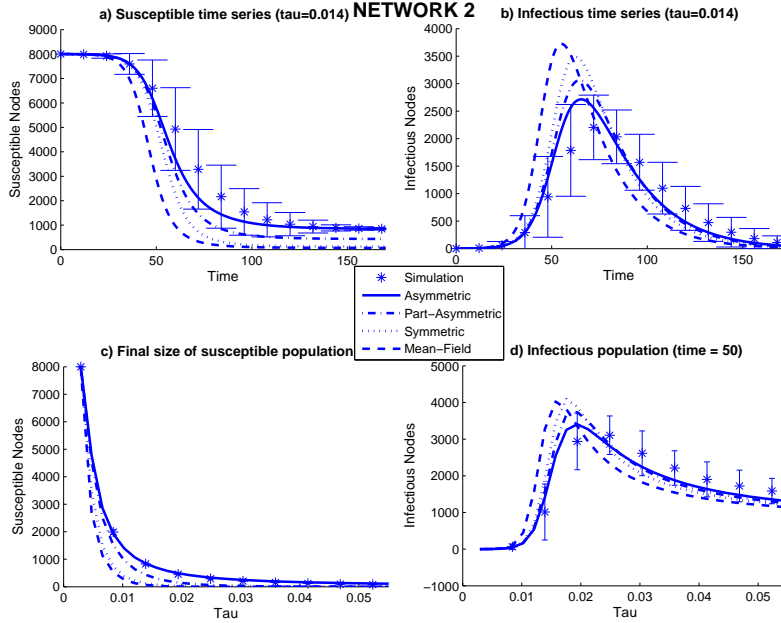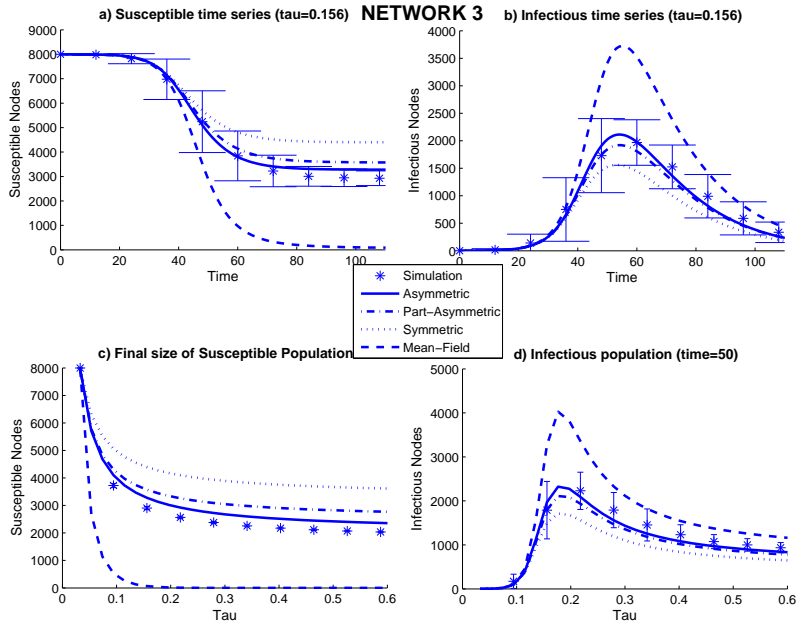
Fig. 6 (Random with triangles) This figure shows the simulation results and model predictions for the random network with added triangles. The mean of 200 simulations is plotted with an asterix where the error bars on the plots indicate a single standard deviation. The other lines indicate the predictions of the four models. The four graphs are: **a)**Susceptible time series for $\tau = 0.014$, $g = 0.05$, **b)**Infectious time series for $\tau = 0.014$, $g = 0.05$, **c)**Final size of the susceptible population and **d)**Infectious population at time interval 50.

    with the conditions in equation (57) we see that the symmetric and part-asymmetric models should be very similar.

– **Network 2 (Random with triangles)**Figure 6 shows that there is a clear difference between the asymmetric and part-asymmetric models. From the discussion in section 7 the difference must be due to the difference in the expressions for $[I \Rightarrow I]$ and also the differences in the triples approximation. It is seen that the asymmetric model is better at predicting the course of the average epidemic on this network.

The part-asymmetric model outperforms the symmetric model. This is to be expected because it accounts for some of the asymmetric structure of the contact network. From table 1 we see that this contact network has $n = n_\rightarrow = 17.29$. Using equation (58) we would estimate $\alpha \approx 0.06$. However, the real value is $\alpha = 0.36$. This illustrates that the approximations in equation (8) are not applicable to this network and that even for large n, α can sometimes be non-zero. This value of α as well as the fact that $\theta \neq 0$ and $\Gamma \neq 0$ explains the discrepancy between the part-asymmetric and symmetric models.
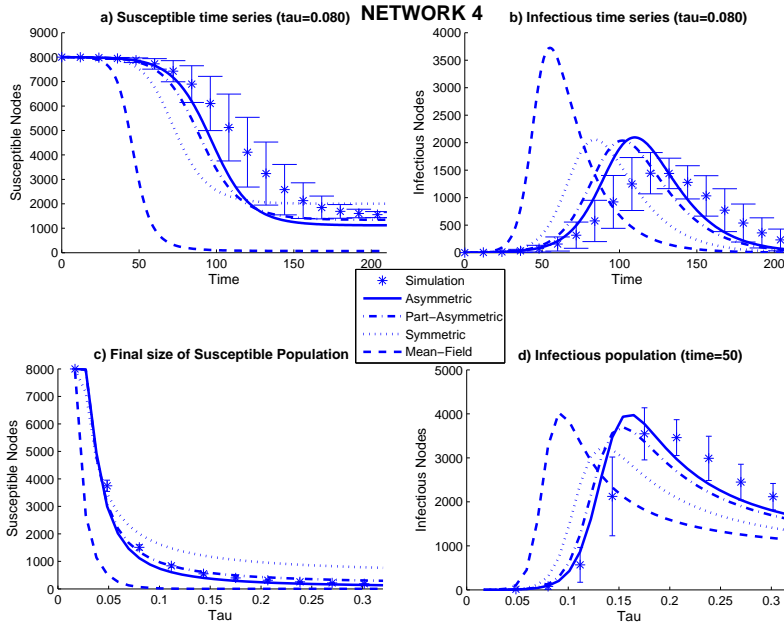
– **Network 3 (River)**

Fig. 7 (River) This figure shows the simulation results and model predictions for the "river" network. The mean of 200 simulations is plotted with an asterix where the error bars on the plots indicate a single standard deviation. The other lines indicate the predictions of the four models. The four graphs are: **a)**Susceptible time series for $\tau = 0.156$, $g = 0.05$, **b)**Infectious time series for $\tau = 0.156$, $g = 0.05$, **c)**Final size of the susceptible population and **d)**Infectious population at time interval 50.

Figure 7 shows that there is a difference between the asymmetric and part-asymmetric models and that the asymmetric model performs slightly better.

For this network, there are essentially no triangles and we have $\alpha = 0.63$. This large value of α explains the difference between the symmetric and part-asymmetric models. It is clear from figure 7 that the part-asymmetric model outperforms the symmetric model.

– **Network 4 (Small world)**This network is part-way between a local network and a random network. We noted at the end of section 3, that our present type of differential equation model is often very poor at predicting epidemics on local contact networks. This network was constructed by starting from a local network and randomly reassigning 20% of all links. Had we reassigned all the links we would have obtained a random network for which these models perform very well. Some discrepancy between the model predictions and the simulation results is therefore expected and it is observed in figure 8.

Here the asymmetric and part-asymmetric models are similar. The difference between the part-asymmetric and symmetric models is due to the non-zero values of α, θ, and Γ.

Fig. 8 (Small world) This figure shows the simulation results and model predictions for the asymmetric small world network. The mean of 200 simulations is plotted with an asterix where the error bars on the plots indicate a single standard deviation. The other lines indicate the predictions of the four models. The four graphs are: **a)**Susceptible time series for $\tau = 0.08$, $g = 0.05$, **b)**Infectious time series for $\tau = 0.08$, $g = 0.05$, **c)**Final size of the susceptible population and **d)**Infectious population at time interval 50.

9 Discussion

We have developed a mathematical model at the pair level to describe the spread of epidemics on contact networks. The primary point of departure from other work in this area is the models applicability to epidemics on asymmetric contact networks. The model for symmetric contact networks is a special case of our model.

In this work the derivation of the closure approximation differs from what has gone before and we believe that this approach provides a degree of clarity that was not previously available. This new derivation enabled the extension of the approximations to asymmetric contact networks. The method of obtaining the closure approximation is a general procedure that is readily applicable to other pair-level models.

We noted that the closure approximation employed here is obtained using the assumption that the number of nodes in a given state is dependent only on the immediate neighbour structure and that higher order dependency is irrelevant. For some network structures this will be a good assumption but for others it will fail to produce good results.

The open network was introduced and we observed that this gives a closed set of pairs. We discussed the completeness relations that result from having a closed set. The completeness relations provide a pair level definition for the open pairs without having to solve the relevant differential equations.

The relationship between the asymmetric and symmetric models was discussed in detail. As part of this analysis, an intermediate model which we termed the part-asymmetric model was also discussed. The part-asymmetric model encompasses a large amount of the asymmetric structure in a greatly simplified form. These models were compared against each other on four contact networks. The behaviour of the models with respect to each other was consistent with what was expected from our analysis.

The predictions of the models were also compared against the results of numerical simulation. This comparison indicated that the asymmetric model generally has superior predictive quality over the symmetric one. For each network the predictions of the part-asymmetric model were in between the predictions of the asymmetric and symmetric models.

We conclude that a pair level model for asymmetric networks can be constructed and that it successfully describes epidemics on a number of contact networks. This model could find applications for diseases on contact networks with asymmetric routes of infection such as such as river networks or transportation networks.

References

1. Anderson, R. M. & May, R. M.: Infectious diseases of humans. Oxford University Press. (1992)
2. Diekmann, O., Heesterbeek, J.A.P., Metz, J.A.J.:The Legacy of Kermack and McKendrick. In: Epidemic Models, their Structure and Relation to Data. (ed. D. Mollison), Cambridge Univ. Press, 95-115 (1995)
3. Ferguson, N. M., Donnelly, C. A. & Anderson, R. M.: The foot-and-mouth epidemic in Great Britain: Pattern of spread and impact of interventions. Science **292**, 1155-1160. (2001)
4. Grenfell, B. T. & Dobson, A. P.: Ecology of infectious diseases in natural populations. Cambridge University Press. (1995)
5. Keeling, M. J.: The effects of local spatial structure on epidemiological invasions. Proc. R. Soc. Lond. **B266**, 859-867. (1999)
6. Kermack, W. O. & McKendrick, A. G.: Contributions to the mathematical theory of epidemics. 1. Proc. R. Soc. Edinb. **A115**, 700-721. (1927)
7. Matsuda, H. N., Ogita A., Sasaki, A., & Satō K.: Statistical mechanics of population: The lattice Lotka-Volterra model. Progress in Theoretical Physics **88**, 1035-1049. (1992)
8. Mollison, D.: Spatial contact models for ecological and epidemic spread. Journal of the Royal Statistical Society. **B 39(3)** 283-326. (1977)
9. Morris, A.J.: Representing spatial interactions in simple ecological models. PhD thesis, Warwick University. (1997)
10. Murray, J. D.: Mathematical Biology. Springer. (2003)
11. Rand, D. A.: Correlation equations for spatial ecologies. In: Advanced ecological theory (ed. J. McGlade), Blackwell Scientific Publishing, 99-143. (1999)
12. Renshaw, E.: Modelling biological populations in space and time. Cambridge University Press. (1991)
13. van Baalen, M.: Pair Approximations for Different Spatial Geometries. In: The Geometry of Ecological Interactions: Simplifying Complexity, eds. Dieckmann, U., Law, R. & Metz, J.A.J., 359-387. (2000)

14. Watts, D. J. & Strogatz, S. H.: Collective dynamics of "small-world" networks.
    Nature Vol 393, 440-442. (1998)